A High Frequency Magnetic Test Bench with Fast Isothermal Measurements for Large Cores

Preferred Topic 1: Topic1 - Devices, Components, Packaging and System Integration
Preferred Subtopic 1: Subtopic 1a - Passive Components
Preferred Topic 2: Topic 2 – Power Converters Topologies
Preferred Subtopic 2: Subtopic 2e - HF Power Converters

Origin: University

Preference: Dialogue (Poster) Session

***Index Terms*— «Core loss», «Experimental testing», «Test bench».**

***Abstract*— This paper presents a magnetic core test-bench developed for high-frequency measurements. The bench is able to perform tests at 1 MHz, 300 V and 20-150 ºC, with temperature precision and high-power capacity suitable for testing voluminous devices. The bench has been tested and the obtained results are presented and discussed.**

I. Introduction

Designing and modeling magnetic components is becoming a crucial task in power electronics. Estimating the power losses for those components is a critical aspect, considering that the necessity to reduce the losses in power applications is increasing.

For cores of any geometry and dimension, the approximation of power losses used for the design are usually obtained by the specification sheet or the datasheet of the material provided by the manufacturer. By this data, an expression to estimate the power losses was obtained, the Steinmetz equation (SE) [1].

$$\overline{P_v} = k f^{\alpha} \hat{B}^{\beta} \tag{1}$$

Where, $\hat{B}$ is the peak flux amplitude, f is the frequency of sinusoidal excitation, $\overline{P_v}$ is the average power loss per unit volume of the core and k, α and β of (1), are constants referred to the core material and temperature, which are obtained empirically.

But those two ways mentioned are not suitable for actual power electronics trends, since power electronics tends to switch mode power supplies (SMPS) without sinusoidal waveforms. Both, the data provided by manufacturers and the estimations obtained by SE are only valid for sinusoidal current waveforms.

For the empirically obtained method, the SE, some adaptations for non-sinusoidal waveforms were done, creating some variants of the base equation. The most popular is the improved generalized Steinmetz equation (2) [2].

$$\overline{P_{\text{iGSE}}} = \frac{k_i}{T} \int_0^T \left|\frac{dB}{dt}\right|^{\alpha} |\Delta B|^{\beta-\alpha}\, dt \tag{2}$$

$$k_i = \frac{k}{2^{\beta-\alpha}\,(2\pi)^{\alpha-1} \int_0^{2\pi} |\cos\theta|^{\alpha}\, d\theta} \tag{3}$$

Where, ΔB is the flux density ripple and k_i is (3). k, α and β are the same constants used in the original equation. These constants, as said before, are referred to the material and variates depending on the temperature of the core, so core losses are related to switching frequency, flux density and temperature. The fact that these constants are the same as those of the SE and as they are deduced from sinusoidal data, opens up the opportunity to transform the database provided by the manufacturer into non-sinusoidal waveforms.

As a solution, a new experimental database is being developed in order to obtain better estimation of core losses. The project, which is called MagNet [3-6], performs tests taking into account different variables. Such as, the ones that are considered by iGSE; frequency, flux density and temperature, and those that are not taken into account; DC magnetization or duty cycle. They test magnetic cores and publish data online, available for anyone.

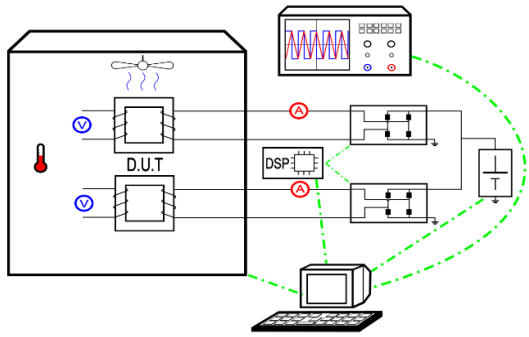

(a)

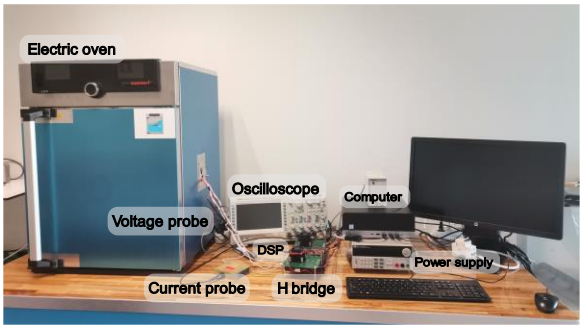

(b)

Figure 1: Test bench (a) distribution schematic and (b) photography of real layout.

An adequate test bench is essential for measure core losses, for validating the commented approximation equations and expand the existent data about the core losses, the test bench from **Figure 1** has been created. The main contributions of this test bench are:

- *Temperature control*; precision and control on the variable temperature whose effect is normally neglected. This test bench can give more detailed information about the tendency of the losses as a function of the temperature. With more precise temperature control while sweeping this variable and expand the existent data to higher temperatures.
- *Precision at flux density*; when testing a point, a flux compensation stage is used to ensure correct measurements, despite the variability of the material and the imperfections caused by the system itself.
- *Isothermal measurements*; the quick measurement method avoids temperature rises between tests and improves the precision on the temperature with the minimization of transient state ensuring tests on steady state.
- *High power capacity*; the utilization of an H bridge, provides the capacity to perform higher powers than similar test benches. Combined with the voluminous space of the oven affords the opportunity to conduct tests to larger cores.

II. Test-bench specifications

The test bench distribution is shown in **Figure 1a** where two equivalent inductors are tested and measured at the same time. For measuring, the two-winding method is used [7], the voltage excitation is applied to a primary winding, where current is measured. The voltage of the secondary winding is measured taking into account the number of turns relation. The hardware used is summed up in **Table I**.

All of the hardware is controlled by a computer via USB and Ethernet communication using a control software created via LabView.

The maximum attainable voltage will depend on the power supply option outlined in **Table I** and the characteristics of the input signal will dictate the appropriate probes. Even if the oven can achieve a temperature of 300 ºC, this is deemed unrealistic, hence the temperature range for practical application has been defined as 20-150 ºC. Furthermore, the bench is configured to perform one test per 10 seconds, as described below.

Table I: Test bench equipment description.

Equipment	Description
H bridge	4x GaN GS66516T-MR, 650 V, 60 A
DUT	EE 55/28/21, 3 turns Litz wire 630x0.1, 60µH
Electric oven	Memmert UF55+, 300 ºC, 53 L
DSP	TMS320F28379D, 200 MHz
Oscilloscope	Rigol DS4024, 200MHz, 4GSa/s, 1 MΩ/50 Ω output
Power supply option 1	ITECH IT6723H, 300 V, 10 A
Power supply option 2	ITECH IT6723G, 600 V, 5 A
Current probe option 1	Iwatsu SS-240A, 10 mA/mV, 30 A_{rms}, DC to 50 MHz
Current probe option 2	T&M Research W-1-01-4 STUD, 100 A/V, 100 A_{rms}, DC to 8 MHz
Voltage probe option 1	Rigol PVP2350, 1:10, 350 V, 350 MHz
Voltage probe option 2	Pintek DP-08VF, 1:200, 800 V_{p-p}, 150 MHz
Thermal Logger	PicoLog USB TC-08 8 Channel temperature datalogger 10S/s

III. Isothermal measurements

Core losses, apart from frequency and flux density, are related to the core temperature. This relation is usually given by the manufacturer as it is shown in the **Figure 2**.

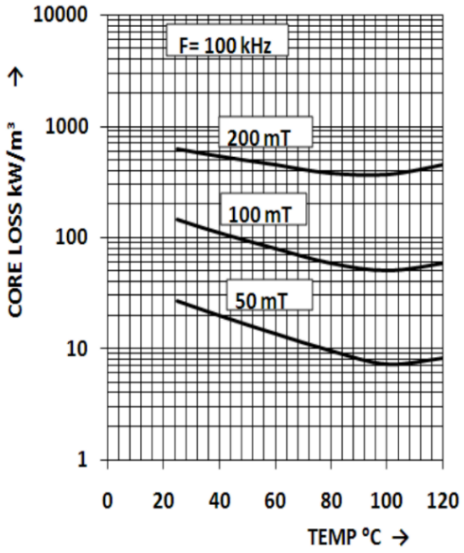

Figure 2: Core losses as a function of the temperature data for CF139 provided by the manufacturer at 100 kHz and for flux densities of 50, 100 and 200 mT [8].

It is clear that the temperature fluctuations can significantly impact in the losses, thus accurate control and monitoring is essential when generating a database. In order to demonstrate how the temperature can change during a test, two tests have been performed, and the recorded temperature results are presented in the **Figure 3**.

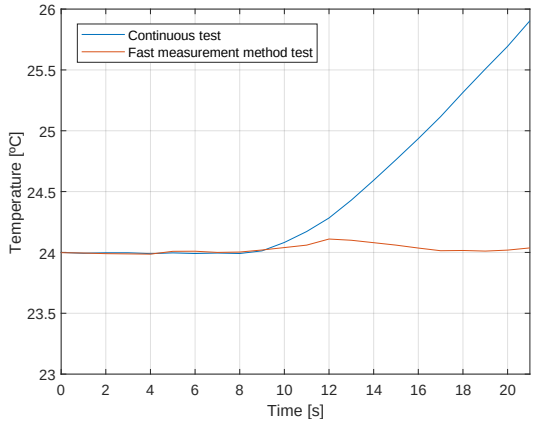

Figure 3: Core temperature evolution in continuous test and fast measurement method test at 100 kHz, 200 mT and 24 ºC. The tests start at second 10 and end approximately at second 20. The first 10 seconds are to show DUTs thermal stability out of test conditions.

Both tests have been performed at the same conditions, and given that the bench operates at a rate of one test per 10 seconds, the duration of the tests is 10 seconds. During the continuous test, the DUT was continuously excited. As a result, the losses generated caused core temperature to rise noticeably, which, in conjunction with the data in **Figure 2**, a variation of approximately 2 ºC at 24 ºC (**Figure 3**), can suppose a variation of 2 % of power loss for the CF139 material. At higher frequencies, the difference caused by the temperature rise is more pronounced. So, in a continuous test, for a correct measurement, a considerable relaxation time will be necessary in order to keep a stable testing point temperature, making the bench slower.

A similar effect is reported in the test bench of MagNet [3-6]. In that case, the DUT is submerged in an oil bath to keep it at the same temperature as the oil. The oil is in a water tank and it is used to control the temperature [9]. During the tests, after 15 minutes they reported a variation of 5 ºC in the DUT. The temperature variation is lower in that case because of the oil bath. The power necessary to increase the temperature in the DUT and the oil is higher than only in the DUT. Even so, in some cases 5 ºC of difference still produces a grade of imprecision.

To avoid those problems, the fast isothermal measurements are proposed. These fast measurements consist on doing the test in some milliseconds and having a relaxation time between tests of some seconds. **Figure 3** illustrates that there is a slight temperature rise caused by the test, which is quickly corrected by the fan built-in the oven. The fan facilitates forced convection around the DUT during the relaxation time and counteracts the temperature increase.

It is logical to infer that reducing the test time will result in a lower temperature rise. While this is true, there is a fundamental limitation that renders it impossible to reduce the test time to a single period, which is the transient state.

As the power loss measurements need to be done in steady state, it is of the upmost interest to achieve steady state as fast as possible to reduce the temperature rise. The evolution of the transient state in a normal test is shown in **Figure 4a**. It is clearly seen that the initial excitation generates a bias current which must fall to 0 amperes before reaching a steady state, so a longer test is necessary.

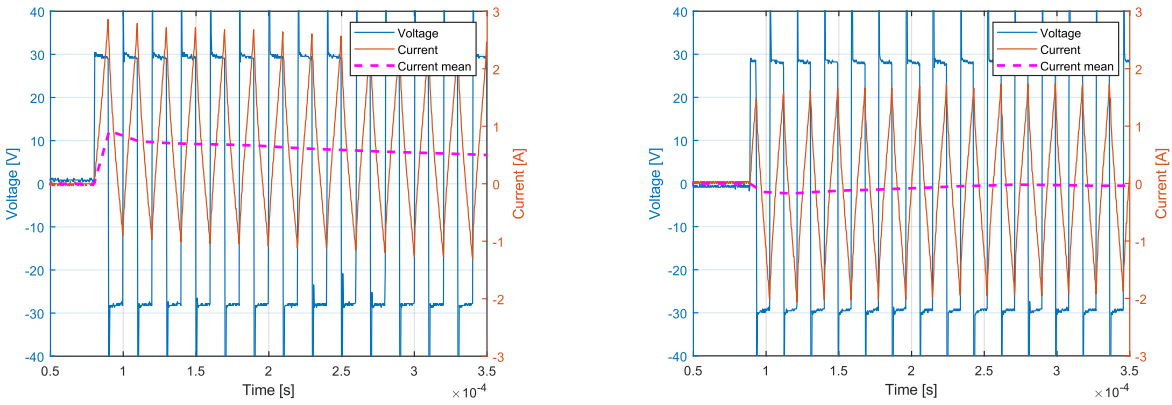

(a) (b)

Figure 4: Voltage, current and average current evolution in (a) normal test start and (b) transient minimization start. Tests done at 25 ºC, 50 kHz and 150 mT.

In **Figure 4b** an alternative initial waveform is shown, where the half of the first semi-period is cut off, minimizing potential bias current sources and maintaining mean current around 0 all the time. The same technique is applied to the last semi-period to ensure that the current mean is near 0 and is ready for the following test.

To ensure steady state is always reached, the initial and final periods are modified as explained above, and 1000 periods are performed every test.

IV. Flux density compensation

In this section is explained why a flux compensation algorithm is needed and how it is implemented.

Due to the direct effect of the switching frequency and the flux density in the core losses, accuracy when setting the test point is essential. In the case of the frequency, as it is controlled by the microcontroller with a resolution of 200 MHz, in the frequency range of 1 MHz the error will be lower than 0.5 %. In the case of the flux density, this depends on many different aspects.

Since the flux density cannot be measured directly, it was obtained from the available electric measurement. Firstly, the characteristic relation between current and voltage of the inductance is taken (4) [10] and current by the inductance is defined as the integral of the inductor voltage in time.

$$V_L = L \cdot \frac{dI_L}{dt} \tag{4}$$

$$\int V_L \, dt = L \, I_L \tag{5}$$

The following magnetism relations are taken too; the relation between magnetic flux, area and flux density (6) obtained by Gauss's law for magnetism [11], Hopkinson's law (7), and an equation derived from Hopkinson's law (8) [12].

$$\Phi = B_c \cdot A_c \tag{6}$$

$$\mathcal{F} = \Phi \cdot \mathcal{R} \tag{7}$$

$$N \cdot i = \mathcal{F} \tag{8}$$

Combining and simplifying those equations, the following equation (9) can be deduced.

$$\mathcal{R} = \frac{N \, I_L}{B_c A_c} \tag{9}$$

The reluctance (10) and the inductance (11) of a uniform magnetic circuit are taken too.

$$\mathcal{R} = \frac{l}{\mu \, A} \tag{10}$$

$$L = \frac{\mu \, N^2 A}{l} \tag{11}$$

Combining those two definitions, reluctance can be defined in the following form (12).

$$\mathcal{R} = \frac{N^2}{L} \tag{12}$$

Taking into account both expressions of reluctance, equalizing them and simplifying flux density can be defined in this form (13).

$$B_c = \frac{L \, I_L}{N A_c} \tag{13}$$

Now replacing the inductance value multiplied with the current in the expression (5), the following expression (14) can be deduced.

$$\int V_L \, dt = N \, A_c \, B_c \tag{14}$$

$$V_L = N\, A_c \frac{dB_c}{dt} \qquad (15)$$

There, it can be deduced that for any voltage waveform applied to the inductance, the flux density in the core will be proportional to the voltage integral. For the observed cases on the test bench, i.e., for square voltage signals, it is obtained that the flux density will be triangular, as it is shown in the **Figure 5**.

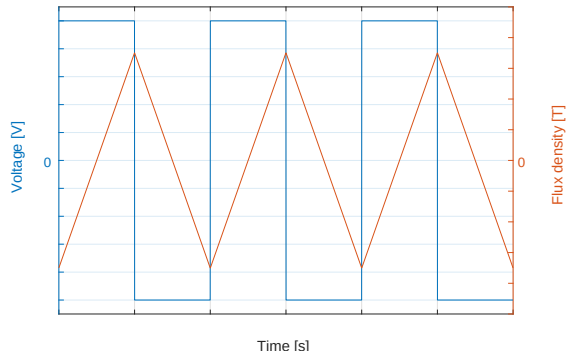

Figure 5: Flux density theoretical evolution in an inductance for a square wave voltage excitation.

Taking a half period as a time frame (dt); while voltage on the inductor is constant and positive (V_L), the flux density is rising, and the flux density change (dB_c) is the flux density ripple. Replacing those values in (15), the expression (16) is deduced:

$$V_L = N\, A_c \frac{\Delta B_c}{\frac{T_{sw}}{2}} \qquad (16)$$

That can be rewritten the following way:

$$V_L = 4\, N\, A_c\, f_{sw} \widehat{B_c} \qquad (17)$$

So, for a defined component with a number of turns and an effective area, every test point with a frequency and a peak flux density will need a certain voltage that will be calculated by the expression (17).

However, for several reasons, the flux density may vary from the desired one. To take a closer look, we will rely on the expression (15), where, the coupling of the turns and the effective area of the core are assumed to be ideal.

The variable that has the potential to introduce errors in flux density is voltage. This error can be attributed to the deviations in the theoretical voltage used in calculations; either by the amplitude of waveform or by the fluctuations in the waveform. The amplitude errors can be produced by; the voltage drop in the wire in between of the converter and the tested device, the coupling between the winding used for testing and the winding used for measuring or the inaccuracy of the measurement probe. The fluctuations, on the other hand, are produced by the switching.

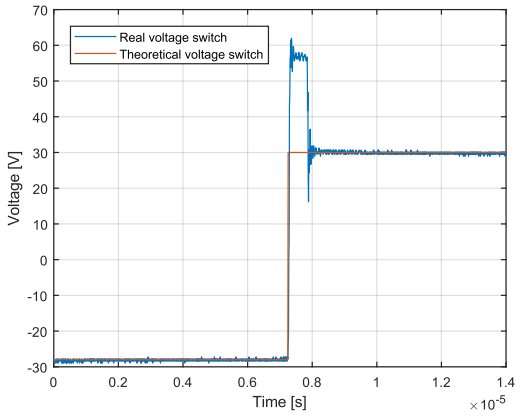

Figure 6: Ideal square voltage wave switching vs real voltage switching.

Figure 6 illustrates, by reasons beyond the focus of this paper, in the deadtime, how the waveform varies from the theoretical one used to do calculations. Knowing this, a simple flux-density compensation algorithm is implemented.

Taking the proportionality between the flux-density and the voltage (17) into account, the error between the desired and measured flux densities are calculated. If there is an error greater than -/+2 %, a correction factor based on the proportionality of flux and voltage is obtained and applied to compensate flux density. The test point is repeated until achieving the desired flux density.

V. Test-bench validation

In this section the test bench is validated to ensure that the data obtained by the bench is reliable. Firstly, the measured waveforms are checked. Secondly, precision and reliability of test are validated. Lastly, obtained results and conclusions are presented.

The square wave voltage output and the current response of the inductor are measured to check the correct functioning of the bench **Figure 7a**. With the measured data, the B-H loop is calculated and plotted in **Figure 7b**. In the peaks of the loop, the effect of the imperfect switch can be observed.

After that, a repetitive test has been conducted, where each test point has been tested ten times, in order to compare each result and define the

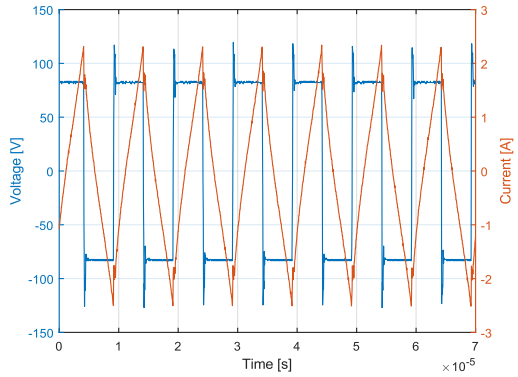

(a)

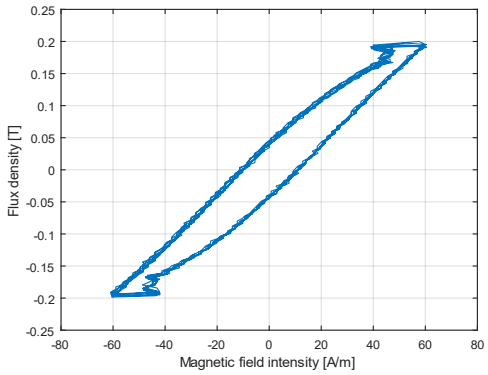

(b)

Figure 7: Single test at 25 ºC, 100 kHz and 200 mT (a) voltage and current waveforms and (b) *B-H* loop.

variability when performing a test. The obtained results are represented in **Figure 8**.

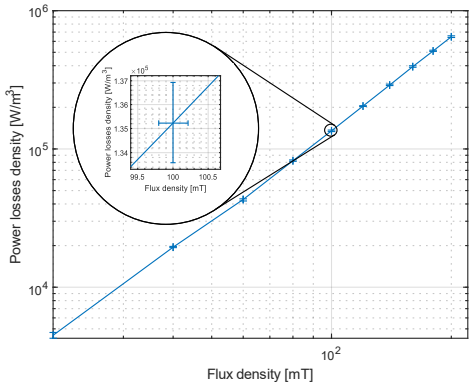

Figure 8: Repetitive test results, density of power losses respect to flux density graph with error bars at 25 ºC and 100 kHz.

In the **Figure 8** the maximum variations or errors are represented with error bars. A zoom of a test point is displayed to see the variability of the flux density and losses easier. There, the maximum error in the flux density is around -/+0.21 % and in the power density is around -/+1.25 %.

Since the test bench allows for testing of two DUTs at the same time, a comparison of the results is also presented in **Figure 9**.

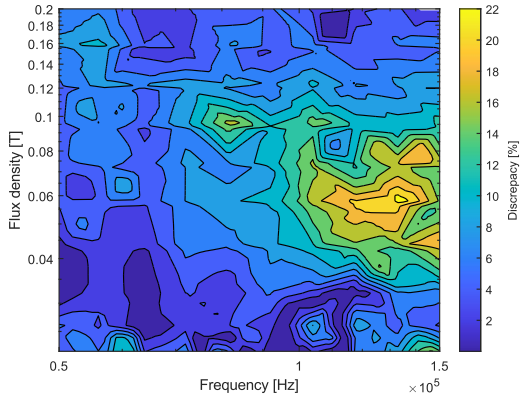

Figure 9: Two DUTs losses discrepancy in function of flux density and frequency, at range of 20-200 mT, 50-150 kHz and at 25 ºC.

There, it is appreciable that there is a maximum discrepancy of 25 % between the two devices. This discrepancy may be attributed to the differences between both devices as well as the inability to perform the exact same test on both devices. The difference between devices, may be due to the differences in the core and in the material, which the suppliers generally quantify as variability, ranging from -20 to +30 % [8], of the magnetic properties. The inability to perform the same test point is caused by the uneven effects of the H bridges in square waves, which result in similar but not equal temperature and flux-density test points.

Also, it is important to mention that the waveforms of the current and the voltage worsen as the test bench is pushed to the limits. In a comparison between **Figure 7a** and **Figure 10** it can be observed how waveforms degrade when commutation frequency increases.

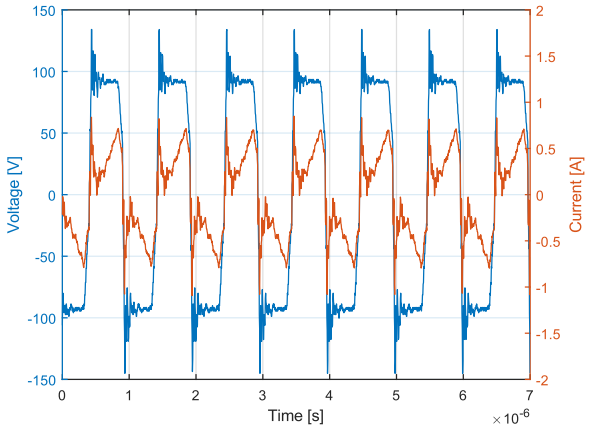

Figure 10: Inductors current response for a 1 MHz square wave voltage, 25 mT and 25 ºC.

As it can be seen in the **Figure 10** the test bench is able to oscillate in 1 MHz, the period time is 1 µs. Due to the current values and the short time involved in oscillating at 1 MHz, the deadtime percentage had to be increased, for the correct functioning of the H bridge.

Lastly, some tests were done to see and compare the obtained results with the approximations obtained via iGSE. To do so, some test points were tested at the same temperature, getting datasets like in **Figure 11**.

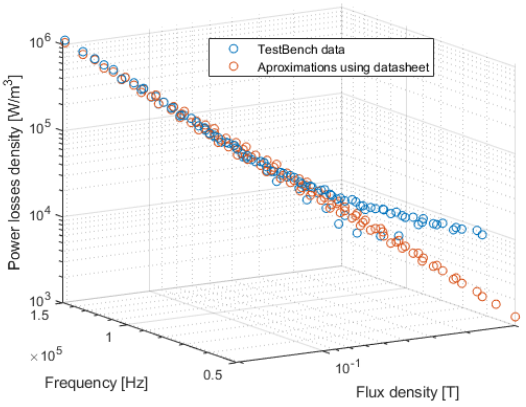

Figure 11: Test bench isothermal power losses results in function of flux density and frequency at 20-200 mT, 50-150 kHz and 25 ºC.

It is appreciable that even if they do not match exactly, the datasets exhibit a similar tendency. The most discrepancy occurs at low flux density and low frequencies where system related issues such as deadtime may lead to non ideal waveforms and accuracy loss. Hence, the bench reliability is higher at high frequencies and flux densities. The test has been repeated in other temperatures to see the effect of the temperature in the approximations.

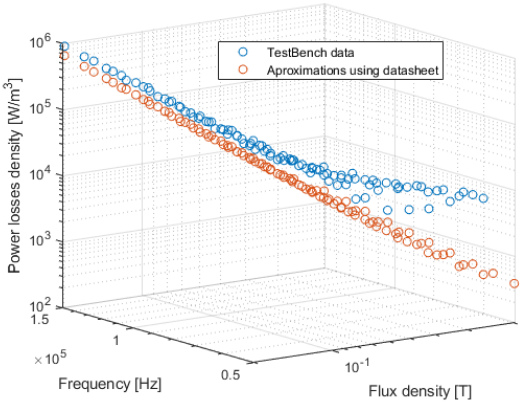

Figure 12: Test bench isothermal power losses results in function of flux density and frequency at 20-200 mT, 50-150 kHz and 100 ºC.

Figure 12 illustrates that at a temperature of 100 ºC, the tendency observed in the previous case was still evident, with the estimations continuing to be true. However, it was also observed that the degree of error had increased, and the two datasets did not align as closely. Nonetheless, the tendency at high frequencies and flux densities remained consistent. Similar to the previous case, the tendency in the losses was disrupted at low frequencies and flux densities, likely due to the same underlying factors.

The last two cases were studied at points were data used to obtaining an approximation were known. Another test was done at 50 ºC, linearly interpolating data at 25 ºC and 100 ºC and obtaining k, α and β values for study temperature. At a temperature of 50 ºC, the obtained result was found to be similar to the two previous cases, indicating that a might be an adequate approach to estimate losses at other temperatures. If the study case is out of the data range, an extrapolation is needed, and to examine the impact on the approximations an additional temperature was studied. For the **Figure 13**, the values of k, α and β were extrapolated for 150 ºC.

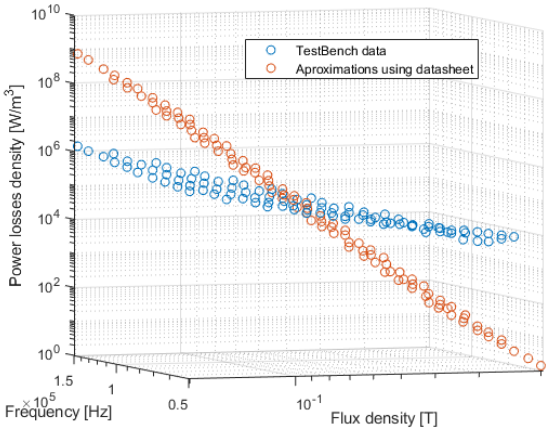

Figure 13: Test bench isothermal power losses results in function of flux density and frequency at 20-200 mT, 50-150 kHz and 150 ºC.

In the **Figure 13** it is clearly seen that the predictions and the test bench data do not follow the same tendency due to the extrapolations done.

VI. Conclusion

The aim of this work is to highlight the importance of having a diverse database for an accurate design of the magnetic devices, and the precision needed while generating the database. The creation of such database can also aid in the development of a better understanding in magnetic loss phenomena or improvements in magnetic loss models.

The temperature effects are usually not considered in the design, due to the lack of information. As seen in the previous part, the

approximations between 25 ºC and 100 ºC are reliable because the data is available, but if the temperature to examine is above that range, the loss predictions quickly become unreliable due to the extrapolations. So, a database with a larger range is needed. This test bench fulfils this requirement by testing the core in a wide temperature range with an adequate resolution and ensuring isothermal tests by testing only 1000 periods.

As said before, ensuring the accuracy of the tested points is crucial to obtain reliable results and avoid errors. To achieve this, a high degree of precision is required during the testing process. For this test bench, a precision of 2 % in flux density was achieved, assuming a good coupling of the turns and core area provided by the suppliers. Concerning the temperature precision, an isothermal measurement method was employed to minimize the temperature rise during tests. Furthermore, the core temperature is measured before every test and the control system waits until the temperature reaches within -/+2 ºC of the desired value before performing the test, resulting in a precision of -/+ 2 ºC for the test bench.

Lastly, using an H bridge instead of a power amplifier [13], like in the bench of MagNet, provides the capacity to test at high power levels, which in turn enables testing larger volume cores. Within such cores, the impact of geometrical and dimensional factors [9] becomes apparent on core losses, but these effects are neglected in the designing process. So, the test bench opens up the opportunity to study the impact of geometrical core parameters in losses, generating much needed insight in this topic.

REFERENCES

[1] E. C. Snelling, *Soft Ferrites, Properties and Applications*. 2nd edition, Butterworths, 1988.

[2] J. Mühlethaler, J. Biela, J. W. Kolar and A. Ecklebe, "Improved Core Loss Calculation for Magnetic Components Employed in Power Electronic Systems," *IEEE Transactions on Power Electronics*, vol. 27, no. 2, pp. 964-973, 2011.

[3] D. Serrano et al., "Neural Network as Datasheet: Modeling B-H Loops of Power Magnetics with Sequence-to-Sequence LSTM Encoder-Decoder Architecture," *IEEE 23rd Workshop on Control and Modeling for Power Electronics (COMPEL)*, 2022.

[4] H. Li et al., "MagNet: an Open-Source Database for Data-Driven Magnetic Core Loss Modeling," *IEEE Applied Power Electronics Conference (APEC)*, 2022.

[5] E. Dogariu et al., "Transfer Learning Methods for Magnetic Core Loss Modeling," *IEEE 22nd Workshop on Control and Modeling for Power Electronics (COMPEL)*, 2021.

[6] H. Li et al., "MagNet: A Machine Learning Framework for Magnetic Core Loss Modeling," *IEEE 21st Workshop on Control and Modeling for Power Electronics (COMPEL)*, 2020.

[7] E. Stenglein et al., "GaN-Half-Bridge for Core Loss Measurements Under Rectangular AC Voltage and DC Bias of the Magnetic Flux Density," *IEEE Transactions on Instrumentation and Measurement*, vol. 69, no. 9, pp. 6312-6321, 2020.

[8] TDK, "Ferrites and accessories EE80/38/20 Core" October 2022. [Online]. Available: https://www.tdk-electronics.tdk.com/inf/80/db/fer/e_80_38_20.pdf

[9] D. Serrano et al., "Why MagNet: Quantifying the Complexity of Modeling Power Magnetic Material Characteristics," TechRxiv. Preprint. Available: https://doi.org/10.36227/techrxiv.21340989.v3

[10] W. G. Hurley, W. H. Wölfle, *Transformers and Inductors for Power Electronics: Theory, Design and Applications*, New Jersey: John Wiley & Sons, 2013.

[11] T. L. Chow, "Gauss' law for the Magnetic Field," *Electromagnetic Theory: A modern perspective*, London, Jones & Barlett, 2006, p. 134.

[12] J. Hopkinson, "Magnetisation of Iron," *Philosophical Transactions Royal Society of London*, vol. 176, p. 455–469, 1885.

[13] Test Equipment Solutions Ltd, "Model 25A250A amplifier," [Online]. Available: https://www.testequipmenthq.com/datasheets/AMPLIFIER%20RESEARCH-25A250A-Datasheet.pdf